# Spin Density and Cluster Dynamics in Sc3N@C80− upon [5,6] Exohedral Functionalization: An ESR and DFT Study

**7 AUTHORS**, INCLUDING:

Anastasia Pykhova
Lomonosov Moscow State University
**2** PUBLICATIONS **10** CITATIONS

SEE PROFILE

José Rivera
Pontificia Universidad Catolica de Puerto R…
**23** PUBLICATIONS **701** CITATIONS

SEE PROFILE

Alexey A Popov
Leibniz Institute for Solid State and Materia…
**188** PUBLICATIONS **3,410** CITATIONS

SEE PROFILE

Luis Echegoyen
University of Texas at El Paso
**445** PUBLICATIONS **13,108** CITATIONS

SEE PROFILE

# Spin Density and Cluster Dynamics in $Sc_3N@C_{80}{}^-$ upon [5,6] Exohedral Functionalization: an ESR and DFT Study

Bevan Elliott,[a] Anastasia D. Pykhova,[b,c] Jose Rivera,[a] Claudia M. Cardona,[a] Lothar Dunsch,[c] Alexey A. Popov,[b,c]* and Luis Echegoyen[d]*

Department of Chemistry, Clemson University, Clemson, SC 29634-0973, United States; [a] Chemistry Department, Moscow State University, 119992 Moscow, Russian Federation; Leibniz-Institute for Solid State and Materials Research, Department of Electrochemistry and Conducting Polymers, 01069 Dresden, Germany; Department of Chemistry, University of Texas at El Paso, El Paso, Texas 79968-0519, United States;

**Abstract**

A radical-anion of [5,6]-pyrrolidine-$Sc_3N@C_{80}$ is generated both chemically and electrochemically and studied by ESR spectroscopy. The rotation of the $Sc_3N$ cluster is shown to be frozen on the ESR timescale, resulting in non-equivalent Sc atoms with hyperfine coupling constants noticeably smaller than in the radical anion of the pristine $Sc_3N@C_{80}$, but larger than in any other derivatives of $Sc_3N@C_{80}$. Experimental ESR studies are supported by extended DFT calculations of the cluster rotational pathways, spin density distribution and hyperfine coupling constants.

## Introduction

Since its discovery in 1999, $Sc_3N@C_{80}$ with icosahedral cage symmetry remains the third most abundantly produced fullerene (after $C_{60}$ and $C_{70}$) and the most abundant endohedral metallofullerene (EMF).[1] The high availability and enhanced stability as compared to conventional EMFs has made $Sc_3N@C_{80}$ the preferred compound to probe the electronic, chemical and physical properties of EMFs.[2, 3] The ESR studies of both chemically and electrochemically produced anion-radical $Sc_3N@C_{80}^-$ revealed that three equivalent scandium atoms yield a 22-line hyperfine pattern with a coupling constant (hfcc) of 55.6 G.[4-6] Among all the Sc-based EMF radicals known so far, including $Sc@C_{82}$,[7, 8] $Sc@C_{84}$,[9] $Sc_3C_2@C_{80}$,[7] as well as the charged states of $Sc_3N@C_{68}$[10, 11] and $Sc_4O_2@C_{80}$,[12] this $a(^{45}Sc)$ value is surpassed only by the recently studied cation-radical of $Sc_4O_2@C_{80}$. The large hfcc indicates that the spin density in $Sc_3N@C_{80}^-$ is localized primarily on the $Sc_3N$ cluster, in accord with the results of the computational studies.[13, 14]

The potential applications of EMFs (e.g., in photovoltaic[15] or medicine[16-20]) usually require derivatization of pristine EMF compounds to improve solubility or introduce functional groups; thus the influence of chemical modification on the electronic and structural properties of EMFs must be thoroughly studied. Exohedral derivatization of EMFs partially saturates the fullerene $\pi$-system and hence substantially changes the way the endohedral cluster interacts with the carbon cage. Redistribution of the frontier orbitals as well as a change of the spatial distribution of the metal-cage bonding sites result from the $\pi$-system saturation. These changes can also modify the internal dynamics of the cluster (e.g., single-crystal X-ray diffraction studies show that free rotation of the $Sc_3N$ cluster in $Sc_3N@C_{80}$ is hindered for the derivatives[21-30]). ESR spectroscopy is an especially convenient tool to address these phenomena since hyperfine

structure strongly depends on the extent of the spin population on metal atoms, whereas the number of equivalent/non-equivalent metal atoms provides information on the cluster dynamics. In particular, hindered rotation of the $Sc_3N$ and $Y_3N$ clusters was revealed by ESR spectroscopy for the radical anions $Sc_3N@C_{80}(CF_3)_x^-$ ($x$ = 2, 10, 12),[6, 28] $Sc_3N@C_{80}(CF_3)_2^{3-}$,[6] and [5,6]-pyrrolidino-$Y_3N@C_{80}$,[31] whereas the decrease of the $a(^{45}Sc)$ values in the $Sc_3N@C_{80}(CF_3)_x^-$ series indicates redistribution of the LUMO from the cluster in $Sc_3N@C_{80}$ to the carbon cage in polytrifluoromethylated derivatives.[28] ESR studies of the cycloadducts of $Sc_3C_2@C_{80}$ also proved that rotation of the $Sc_3C_2$ cluster is hindered after derivatization.[32-35] Although dipolar cycloaddition is among the most ubiquitous derivatization techniques used to prepare many derivatives of $Sc_3N@C_{80}$,[25, 36-44] the influence of the pyrrolidine ring on the endohedral cluster is not well characterized, especially for the charged states.

In this work, we report an ESR spectroscopic study of the radical anion of a pyrrolidine cycloadduct of $Sc_3N@C_{80}$ and an assignment of the spectrum based on DFT calculations. A complicated hyperfine structure produced by non-equivalent Sc atoms unambiguously proves the reduction of the cluster symmetry and the hindrance of its rotational motions. In addition, the total spectral width is considerably smaller than that of the anion of the pristine $Sc_3N@C_{80}$, suggesting a partial transfer of spin from the $Sc_3N$ cluster to the carbon cage induced by the cycloaddition.

### Experimental and Computational Details

A [5,6]-*n*-ethyl-pyrrolidino-$Sc_3N@C_{80}$ derivative was synthesized in the same way as described earlier[44] using the $Sc_3N@C_{80}$ provided by Luna Innovations, Inc. Chemical reductions were performed in a glass-blown two-compartment cell with a connected EPR tube using potassium

4

metal in THF solution. Pure [5,6]-pyrrolidino-$Sc_3N@C_{80}$ was placed in one compartment of the cell, and potassium metal in the other, and the cell was pumped under high vacuum. Dry THF was then vapor-transferred into the cell, and the connection to the vacuum line flame-sealed. The compound was reduced by repeated contact of the THF solution with the potassium metal, after which the solution was transferred into the EPR tube. The first derivative X-band spectra were recorded using a Bruker EMX spectrometer.

Preliminary optimization of the molecular structures was performed using PBE exchange-correlation functional[45] and TZ2P-quality basis set (full-electron {6,3,2}/(11s,6p,2d) for C, N, and SBK-type effective core potential for Sc atoms with {5,5,4}/(9s,9p,8d) valence part implemented in the PRIRODA package.[46, 47] More extended computations of the lowest energy conformers of the anion (optimization, IRC) were then performed with the Λ2m basis set {4,3,2}/(12s,8p,4d) for cage carbon atoms and pyrrolidine ring, the Λ3 basis set {5,4,3,2,1}/(14s,10p,5d,4f,3g) for N, and Λ33 basis {10s,9p,7d,5f,3g,1h}/ {27s,22p,16d,10f,8g,4h) for Sc. For hfcc and energy calculations along the IRC trajectories (the values in the Table 1 and Figure 3) the basis for carbon atoms was extended to Λ2 {4,3,2,1}/(12s,8p,4d,2f).[48] The structures, trajectories and isosurfaces were visualized with VMD.[49]

**Results and Discussion**

The electrochemical study of the compounds was reported earlier and showed that the derivative exhibits reversible reduction at the potential of −1.18 V versus $Fe(Cp)_2^{+/0}$ couple,[37] which is 0.08 V more positive than the first reduction of $Sc_3N@C_{80}$ at −1.26 V.[5] Electrochemical reversibility of the first reduction step indicates that the radical anion of [5,6]-*n*-ethyl-pyrrolidino-$Sc_3N@C_{80}$

is sufficiently stable in solution at room temperature and hence can be studied by electron spin resonance spectroscopy.

The ESR spectrum of the radical anion produced by chemical reduction (potassium metal in a THF solution) of the pyrrolidino-derivative is shown in Figure 1. An electrochemical reduction of the $Sc_3N@C_{80}$ derivative in *o*-dichlorobenzene yielded an equivalent ESR spectrum (see Supporting Information for further details). Owing to the $I = 7/2$ spin of $^{45}Sc$, a rich hyperfine structure in the spectrum of the radical anion of the [5,6]-pyrrolidino-$Sc_3N@C_{80}$ can be expected, especially if Sc atoms have large spin population as found earlier in the radical anions of $Sc_3N@C_{80}$[4] and $Sc_3N@C_{80}(CF_3)_{2,10,12}$.[6, 28] In the $Sc_3N@C_{80}^-$, three equivalent Sc atoms give rise to the characteristic ESR spectrum with 22 main lines and a number of second-order features caused by the large $^{45}Sc$ coupling constant of 55–57 G. In contrast to the 22-line spectrum of $Sc_3N@C_{80}^-$, the spectrum of [5,6]-pyrrolidino-$Sc_3N@C_{80}^-$ exhibits many more lines with the total hyperfine pattern spanning the field range of 535 G, more than two times narrower than the spectral width of the non-functionalized $Sc_3N@C_{80}^-$ (ca 1100 G). The g-factor is significantly shifted to 1.9972, and the linewidth, 2.8 G, is almost half that of the pristine $Sc_3N@C_{80}^-$. A second-order simulation accounting for all spectral lines proved that the symmetry of the cluster has been reduced by the cycloaddition reaction, resulting in one scandium that is non-equivalent to the other two. The $a(^{45}Sc)$ hfc constant of the single scandium is 9.6 G, whereas the two equivalent Sc atoms have a hfcc of 33.4 G. The study of the radical anion of pristine $Sc_3N@C_{80}$ under the same conditions yielded a spectrum with $a(^{45}Sc)$ value of 56.0 G, a linewidth of 5.5 G, and a g-factor of 1.9923. The reduced symmetry of the $Sc_3N$ cluster caused by the cycloaddition in the pyrrolidino-$Sc_3N@C_{80}$ is reminiscent of the analogous situation found in the mono- and trianion of $Sc_3N@C_{80}(CF_3)_2$[6] as well as in the fulleropyrrolidine adducts of $Sc_3C_2@C_{80}$.[34, 35] In

these compounds, exohedral derivatization also hindered rotation of the endohedral cluster, resulting in more complex hyperfine structure. In $Sc_3N@C_{80}^-$ and $Sc_3C_2@C_{80}$, the clusters are rotating almost freely at room temperature, and hyperfine coupling constants Sc atoms are averaged over time.
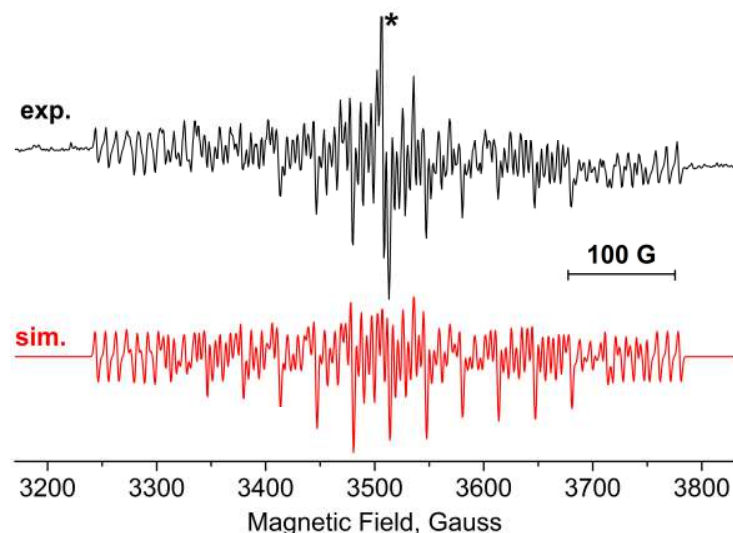


**Figure 1.** Experimental (top) and simulated (bottom) X-band ESR spectra of the chemically reduced mono-anion of [5,6]-pyrrolidino-$Sc_3N@C_{80}$. The asterisk denotes an impurity.

To analyze the influence of the cycloaddition on the molecular structure and electronic properties of [5,6]-pyrrolidino-$Sc_3N@C_{80}$, we performed DFT calculations of this derivative in the neutral and charged states. Cycloaddition reduces the symmetry of the carbon cage and provides a possibility of large energy variations depending on the cluster orientation within the carbon cage. To address this dependence in the most possible detail we generated 52 conformers of [5,6]-pyrrolidino-$Sc_3N@C_{80}$ fusing the pyrrolidine ring to all non-equivalent 5/6 edges in the lowest energy $C_3$- and $C_s$-symmetric conformers of $Sc_3N@C_{80}$ (see ref. 13 for a detailed study of

7

Sc$_3$N@C$_{80}$) and then performed DFT optimizations. The procedure resulted in 45 non-equivalent conformers for the neutral molecule and 41 conformers for the anion. In all of these structures the pyrrolidine nitrogen atom was placed over the cage pentagon; inversion of the ring increases the energy by ca 5 kJ/mol. The energy range covered by the conformers (65 and 75 kJ/mol for the neutral molecule and anion, respectively) is much larger than that found for different positions of the cluster in the non-functionalized Sc$_3$N@C$_{80}$ (ca 10 and 25 kJ/mol for the neutral and anionic forms) showing that 3D rotation of the cluster is substantially hindered in the cycloadduct.

In the lowest energy conformer (**I**) found in this study for the non-charged [5,6]-pyrrolidino-Sc$_3$N@C$_{80}$, two Sc atoms (denoted hereafter as Sc1 and Sc2) are coordinated near the carbon atoms in the *para*-positions with respect to the C-sp$^3$ atoms, whereas the third Sc atom (Sc3) is facing the carbon atom on the pentagon/hexagon/hexagon junction located on the opposite pole of the molecule (Fig. 2a). This structure agrees well with the single-crystal X-ray diffraction studies of the [5,6] cycloadducts of Sc$_3$N@C$_{80}$[23-26] as well as with earlier computational studies.[14, 36] In the second most stable conformer (**II**, $\Delta E$ = 2.2 kJ/mol) the third Sc atom is facing the 5/6 edge instead of the single carbon atom; otherwise the structure is very similar (Fig. 2b). The relative energy of the third most stable conformer is 13.5 kJ/mol, and all other conformers are densely distributed over the energy range of 13.8–64.8 kJ/mol (see S.I. for more details).
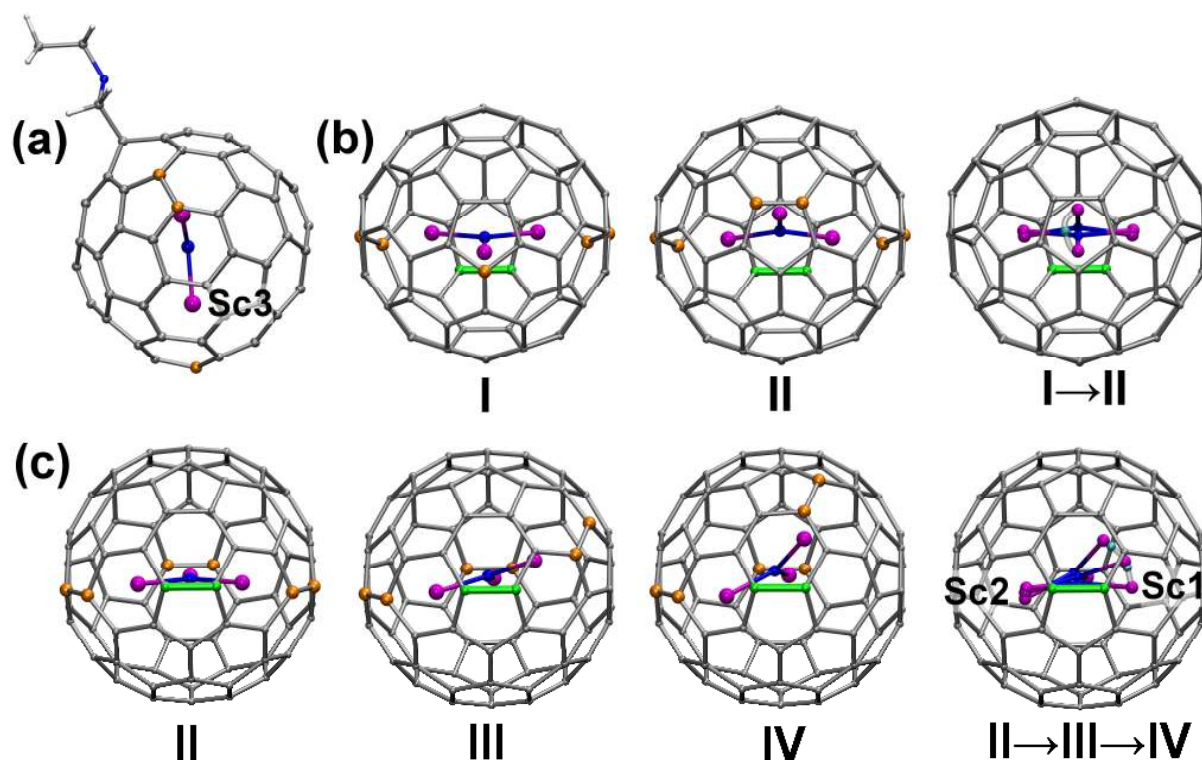
**Figure 2.** DFT-optimized conformers **I–IV** of the anion-radical of [5,6]-pyrrolidino-$Sc_3N@C_{80}$: (a) conformer **I**; (b) conformers **I**, **II**, and the **I→II** IRC trajectory; (c) conformers **II**, **III**, **IV**, and the **II→III→IV** IRC trajectory. For the sake of clarity, the conformers in (b-c) are shown in the orientations where the motion of the Sc atom(s) is seen best, the pyrrolidine ring is omitted, the functionalized 5/6 edge is highlighted in green, and the carbon atoms with the shortest Sc–C distances are highlighted in orange. IRC trajectories are shown with superimposed positions of the $Sc_3N$ cluster in the energy minima, and positions of the most labile Sc atoms in transition states are shown as cyan.

Two lowest energy conformers of the anion with an energy difference of only 2.4 kJ/mol resemble those of the neutral [5,6]-pyrrolidino-$Sc_3N@C_{80}$. The study also revealed that the third and fourth lowest energy conformers (**III**, $\Delta E = 10.4$ kJ/mol; **IV**, $\Delta E = 20.9$ kJ/mol) are related to the conformer **II** and can be obtained from the latter by rotation around the Sc3–N bond (Fig. 2c). The other conformers are noticeably higher in energy (the majority of the structures spans the range of 33–55 kJ/mol) and can be omitted in the analysis of the hfc values.

Table 1 lists DFT-predicted $a(^{45}Sc)$ constants for the conformers **I–IV** as well as for the transition states (TSs) along the pathways between them, and Figure 3 shows relative energies, $a(^{45}Sc)$ constants and Sc spin populations computed along the **I→II→III→IV** intrinsic reaction coordinate (IRC) pathway. The energy profile shows that the barriers along **I→II** and **II→III** trajectories are relatively small (11.5 and 10.6 kJ/mol, respectively); besides, the conformer **III** is found to be only a small bump on the potential energy surface (its energy is 0.2 kJ/mol below the energy of the transition state). The energies of the TS(**III→IV**) and of the conformer **IV** are larger (23.5 and 20.9 kJ/mol, respectively) but still reachable at room temperature. This means that under the conditions of the ESR measurements, the cluster is expected to move rapidly between the four conformers, and adequate interpretation of the ESR spectra must take into account this complex dynamic situation.

$^{45}Sc$ hfcc values are found to be extremely sensitive to the position of Sc atoms (similar results were found before for some other Sc-based EMF radicals). For instance, $a(^{45}Sc1)$ in **II** (27.8 G) is *ca* two times larger than in **I** (12.9 G), although positions of Sc1 and Sc2 are only slightly altered in the **I→II** transition (Fig. 2b). Furthermore, $a(^{45}Sc1)$ increases to 46.5 G in **III**, and then drops down to 14.2 G when Sc1 is further moved to the conformer **IV**. At the same time, $a(^{45}Sc2)$ drops from 27.8 G in **II** to 5.5 G in **IV**, although displacements of Sc2 along the

**II→III→IV** pathway are very small (Fig. 2c). The hfcc of Sc3 at the energy minima does not exceed 6 G irrespective of the conformer, however the largest value (17.2 G) is achieved between **I** and TS(**I→II**). Note that the lowest energy path between $C_s$-symmetric conformers **I** and **II** breaks the symmetry as the Sc3 prefers to move along the 5/6 edges rather than through the middle of the pentagon (Fig. 2b). Computations also showed that inversion of the pyrrolidine ring has almost no effect on the hfc constants.

In general, DFT computations show that the hfc constants of Sc1 and Sc2 are significantly larger than that of Sc3. Averaging the $a(^{45}Sc)$ constants along the **I→II→III→IV** IRC path using temperature Boltzmann factors and taking into account the $C_s$ symmetry of the functionalized carbon cage gives hfc constants of 19.3 G for Sc1/Sc2 and 4.9 G for Sc3 in qualitative agreement with the experimental data (the value for Sc3 is several times smaller than that for Sc1/Sc2). However, DFT-derived $a(^{45}Sc)$ values are almost a factor of 2 smaller than the experimental ones. Similar underestimation was found for $Sc_3N@C_{80}^-$ in ref. [13] and was partially explained by the dynamic effects.[50] Averaging the hfc constant along the molecular dynamics trajectory resulted in a noticeably larger value than that obtained at the same level of theory for a static computation at the energy minimum.[50] Presumably, taking into account dynamic effects in the anion-radical of [5,6]-pyrrolidino-$Sc_3N@C_{80}$ in a more robust manner may improve agreement between experiment and theory, but such a task exceeds the goal of this work.
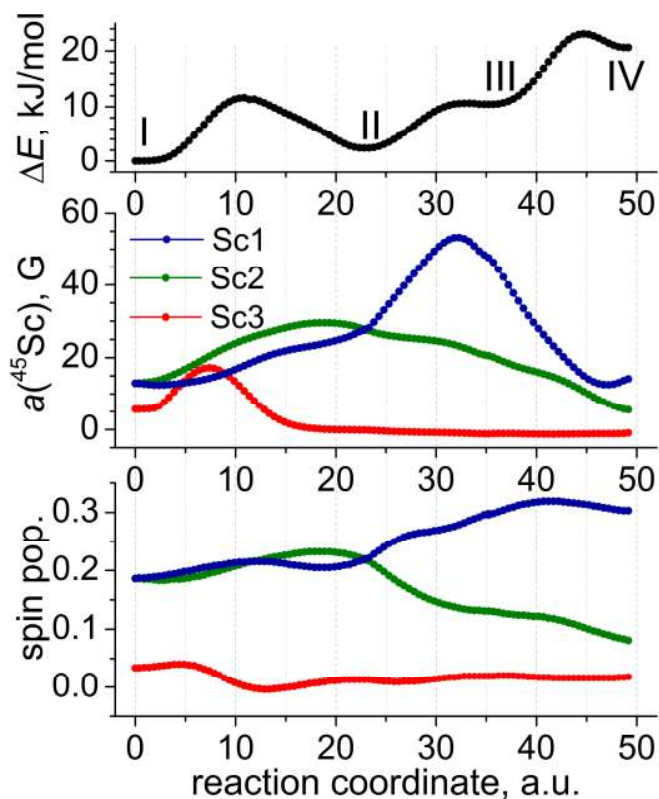
**Figure 3.** Energy (top), $a(^{45}Sc)$ constants (middle) and Sc spin populations (bottom) computed for the radical anion of [5,6]-pyrrolidino-$Sc_3N@C_{80}$ along the **I→II→III→IV** IRC pathway.

**Table 1.** DFT-computed relative energies ($\Delta E$) and $^{45}Sc$ hyperfine coupling constants for selected $Sc_3N$ positions in the radical anion of the [5,6]-pyrrolidino-$Sc_3N@C_{80}$.

| conformer | $\Delta E$, kJ/mol | $a(^{45}Sc1)$, G | $a(^{45}Sc2)$, G | $a(^{45}Sc3)$, G |
|---|---|---|---|---|
| **I** | 0.0 | 12.9 | 12.9 | 5.7 |
| TS(**I→II**) | 11.5 | 17.8 | 24.9 | 10.9 |
| **II** | 2.4 | 27.8 | 27.8 | −0.1 |
| TS(**II→III**) | 10.6 | 52.9 | 22.7 | −1.0 |
| **III** | 10.4 | 46.5 | 20.2 | −1.2 |
| TS(**III→IV**) | 23.5 | 15.0 | 10.7 | −1.2 |
| **IV** | 20.9 | 14.2 | 5.5 | −0.9 |
| aver. (298 K) | | 19.3 | 19.3 | 4.9 |
| exp. | | 33.4 | 33.4 | 9.6 |

Spin populations of Sc atoms in the radical anion of [5,6]-pyrrolidino-$Sc_3N@C_{80}$ also experience noticeable changes depending on the cluster position inside the carbon cage (Fig. 4), but the net population of all Sc atoms remains in the range of 0.40–0.46 (compared to 0.64 in $Sc_3N@C_{80}{}^{-}$[13]). Spin population for Sc3 does not exceed 0.04, and the spin density is mostly localized on the Sc1/Sc2 atoms and the carbon cage near the pyrrolidine addition site (see Fig. 4 for visualization of the spin density in **I** and **II**), which agrees with the results of the earlier computational studies for one of the conformers.[14]
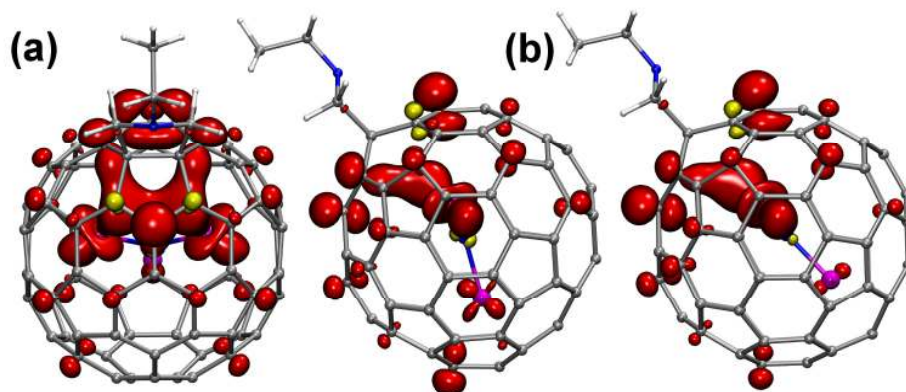


**Figure 4.** Spin-density isosurfaces (at ±0.0016 a.u., red – positive density, yellow – negative density) for the radical anion of [5,6]-pyrrolidino-$Sc_3N@C_{80}$: (a) conformer **I**; (b) conformer **II**. For the sake of clarity, conformer **I** is shown in two orientations.

**Conclusions**

Combined ESR and DFT study of the radical anion of [5,6]-pyrrolidino-$Sc_3N@C_{80}$ shows that cycloaddition imposes a significant impact on the electronic structure and internal dynamics of the $Sc_3N@C_{80}$ core. Partial saturation of the fullerene $\pi$-system at only one 5/6 edge significantly hinders rotational motion of the $Sc_3N$ cluster, and its three Sc atoms are not equivalent on the ESR time scale. The [45]Sc hyperfine coupling constants in the radical anion of [5,6]-pyrrolidino-$Sc_3N@C_{80}$ are noticeably reduced in comparison to those of $Sc_3N@C_{80}^-$, showing that the spin density is shifted from the cluster to the carbon cage. Moreover, chemical functionalization results in the enhanced asymmetry of the spin density distribution, the $a(^{45}Sc)$ constant and spin population of the Sc atom opposing the pyrrolidine ring being ca 4 times smaller than those for the two equivalent Sc atoms coordinated in the vicinity of the pyrrolidine fragment. These results emphasize flexibility and tunability of the electronic structure of $Sc_3N@C_{80}$ and show that relatively small perturbation of the fullerene $\pi$-system results in the significant changes of the frontier orbitals and the cluster dynamics. Based on the experimental electrochemical and ESR spectroscopic studies as well as quantum-chemical computations, we can conclude that cycloaddition stabilizes the carbon cage-based unoccupied MOs, which results in the higher contribution of the carbon cage to the LUMO of the cycloadducts and therefore reduced spin populations and hyperfine coupling constants of Sc atom in comparison to the radical anion $Sc_3N@C_{80}^-$.

**Corresponding Author**

E-mail: a.popov@ifw-dresden.de, echegoyen@utep.edu

## References

1. Stevenson, S.; Rice, G.; Glass, T.; Harich, K.; Cromer, F.; Jordan, M. R.; Craft, J.; Hadju, E.; Bible, R.; Olmstead, M. M., et al. *Nature* **1999,** 401, 55-57.
2. Dunsch, L.; Yang, S. *Small* **2007,** 3, 1298-1320.
3. Chaur, M. N.; Melin, F.; Ortiz, A. L.; Echegoyen, L. *Angew. Chem.-Int. Edit.* **2009,** 48, 7514-7538.
4. Jakes, P.; Dinse, K. P. *J. Am. Chem. Soc.* **2001,** 123, 8854-8855.
5. Elliott, B.; Yu, L.; Echegoyen, L. *J. Am. Chem. Soc.* **2005,** 127, 10885-10888.
6. Popov, A. A.; Shustova, N. B.; Svitova, A. L.; Mackey, M. A.; Coumbe, C. E.; Phillips, J. P.; Stevenson, S.; Strauss, S. H.; Boltalina, O. V.; Dunsch, L. *Chem.-Eur. J.* **2010,** 16, 4721-4724.
7. Yannoni, C. S.; Hoinkis, M.; Devries, M. S.; Bethune, D. S.; Salem, J. R.; Crowder, M. S.; Johnson, R. D. *Science* **1992,** 256, 1191-1192.
8. Suzuki, S.; Kawata, S.; Shiromaru, H.; Yamauchi, K.; Kikuchi, K.; Kato, T.; Achiba, Y. *J. Phys. Chem.* **1992,** 96, 7159-7161.
9. Inakuma, M.; Shinohara, H. *J. Phys. Chem. B* **2000,** 104, 7595-7599.
10. Yang, S. F.; Rapta, P.; Dunsch, L. *Chem. Commun.* **2007**, 189-191.
11. Rapta, P.; Popov, A. A.; Yang, S. F.; Dunsch, L. *J. Phys. Chem. A* **2008,** 112, 5858-5865.
12. Popov, A. A.; Chen, N.; Pinzón, J. R.; Stevenson, S.; Echegoyen, L. A.; Dunsch, L. *J. Am. Chem. Soc.* **2012,** 134, 19607–19618.
13. Popov, A. A.; Dunsch, L. *J. Am. Chem. Soc.* **2008,** 130, 17726-17742.
14. Valencia, R.; Rodriguez-Fortea, A.; Clotet, A.; de Graaf, C.; Chaur, M. N.; Echegoyen, L.; Poblet, J. M. *Chem.-Eur. J.* **2009,** 15, 10997-11009.
15. Rudolf, M.; Wolfrum, S.; Guldi, D. M.; Feng, L.; Tsuchiya, T.; Akasaka, T.; Echegoyen, L. *Chem.-Eur. J.* **2012,** 18, 5136–5148.
16. Wilson, L. J.; Cagle, D. W.; Thrash, T. P.; Kennel, S. J.; Mirzadeh, S.; Alford, J. M.; Ehrhardt, G. J. *Coord. Chem. Rev.* **1999,** 192, 199-207.
17. Dorn, H. C.; Fatouros, P. P. *Nanosci. Nanotechnol. Lett.* **2010,** 2, 65-72.
18. Ananta, J. S.; Wilson, L. J., Gadonanostructures as Magnetic Resonance Imaging Contrast Agents. In *Chemistry of Nanocarbons*, Akasaka, T.; Wudl, F.; Nagase, S., Eds. John Wiley & Sons, Ltd: Chichester, UK, 2010; pp 287-300.
19. Bolskar, R. D., Gadolinium Endohedral Metallofullerene-Based MRI Contrast Agents. In *Medicinal Chemistry and Pharmacological Potential of Fullerenes and Carbon Nanotubes*, Cataldo, F.; Da Ros, T., Eds. Springer Netherlands: 2008; Vol. 1, pp 157-180.
20. Bolskar, R. D. *Nanomedicine* **2008,** 3, 201-213.
21. Wakahara, T.; Iiduka, Y.; Ikenaga, O.; Nakahodo, T.; Sakuraba, A.; Tsuchiya, T.; Maeda, Y.; Kako, M.; Akasaka, T.; Yoza, K., et al. *J. Am. Chem. Soc.* **2006,** 128, 9919-9925.
22. Shu, C.; Slebodnick, C.; Xu, L.; Champion, H.; Fuhrer, T.; Cai, T.; Reid, J. E.; Fu, W.; Harich, K.; Dorn, H. C., et al. *J. Am. Chem. Soc.* **2008,** 130, 17755-17760.
23. Iezzi, E. B.; Duchamp, J. C.; Harich, K.; Glass, T. E.; Lee, H. M.; Olmstead, M. M.; Balch, A. L.; Dorn, H. C. *J. Am. Chem. Soc.* **2002,** 124, 524-525.
24. Lee, H. M.; Olmstead, M. M.; Iezzi, E.; Duchamp, J. C.; Dorn, H. C.; Balch, A. L. *J. Am. Chem. Soc.* **2002,** 124, 3494-3495.

25.    Cai, T.; Slebodnick, C.; Xu, L.; Harich, K.; Glass, T. E.; Chancellor, C.; Fettinger, J. C.; Olmstead, M. M.; Balch, A. L.; Gibson, H. W., et al. *J. Am. Chem. Soc.* **2006,** 128, 6486-6492.
26.    Li, F.-F.; Pinzon, J. R.; Mercado, B. Q.; Olmstead, M. M.; Balch, A. L.; Echegoyen, L. *J. Am. Chem. Soc.* **2011,** 133, 1563-1571.
27.    Shustova, N. B.; Chen, Y.-S.; Mackey, M. A.; Coumbe, C. E.; Phillips, J. P.; Stevenson, S.; Popov, A. A.; Boltalina, O. V.; Strauss, S. H. *J. Am. Chem. Soc.* **2009,** 131, 17630-17637.
28.    Shustova, N. B.; Peryshkov, D. V.; Kuvychko, I. V.; Chen, Y.-S.; Mackey, M. A.; Coumbe, C. E.; Heaps, D. T.; Confait, B. S.; Heine, T.; Phillips, J. P., et al. *J. Am. Chem. Soc.* **2011,** 133, 2672-2690.
29.    Yang, S.; Chen, C.; Lanskikh, M. A.; Tamm, N. B.; Kemnitz, E.; Troyanov, S. I. *Chem.-Asian J.* **2011,** 6, 505-509.
30.    Wang, G.-W.; Liu, T.-X.; Jiao, M.; Wang, N.; Zhu, S.-E.; Chen, C.; Yang, S.; Bowles, F. L.; Beavers, C. M.; Olmstead, M. M., et al. *Angew. Chem.-Int. Edit. Engl.* **2011,** 50, 4658-4662.
31.    Echegoyen, L.; Chancellor, C. J.; Cardona, C. M.; Elliott, B.; Rivera, J.; Olmstead, M. M.; Balch, A. L. *Chem. Commun.* **2006,** 2653-2655.
32.    Iiduka, Y.; Wakahara, T.; Nakahodo, T.; Tsuchiya, T.; Sakuraba, A.; Maeda, Y.; Akasaka, T.; Yoza, K.; Horn, E.; Kato, T., et al. *J. Am. Chem. Soc.* **2005,** 127, 12500-12501.
33.    Kato, T. *J. Mol. Struct.* **2007,** 838, 84-88.
34.    Wang, T.; Wu, J.; Xu, W.; Xiang, J.; Lu, X.; Li, B.; Jiang, L.; Shu, C.; Wang, C. *Angew. Chem.-Int. Edit. Engl.* **2010,** 49, 1786-1789.
35.    Wang, T.; Wu, J.; Feng, Y.; Ma, Y.; Jiang, L.; Shu, C.; Wang, C. *Dalton Trans.* **2012,** 41, 2567-2570.
36.    Pinzyn, J. R.; Cardona, C. M.; Herranz, M. A.; Plonska-Brzezinska, M. E.; Palkar, A.; Athans, A. J.; Martin, N.; Rodriguez-Fortea, A.; Poblet, J. M.; Bottari, G., et al. *Chem.-Eur. J.* **2009,** 15, 864-877.
37.    Cardona, C. M.; Elliott, B.; Echegoyen, L. *J. Am. Chem. Soc.* **2006,** 128, 6480-6485.
38.    Cai, T.; Ge, Z. X.; Iezzi, E. B.; Glass, T. E.; Harich, K.; Gibson, H. W.; Dorn, H. C. *Chem. Commun.* **2005,** 3594-3596.
39.    Pinzyn, J. R.; Plonska-Brzezinska, M. E.; Cardona, C. M.; Athans, A. J.; Gayathri, S. S.; Guldi, D. M.; Herranz, M. A.; Martin, N.; Torres, T.; Echegoyen, L. *Angew. Chem.-Int. Edit. Engl.* **2008,** 47, 4173-4176.
40.    Pinzon, J. R.; Gasca, D. C.; Sankaranarayanan, S. G.; Bottari, G.; Torres, T.; Guldi, D. M.; Echegoyen, L. *J. Am. Chem. Soc.* **2009,** 131, 7727-7734.
41.    Wolfrum, S.; Pinzon, J. R.; Molina-Ontoria, A.; Gouloumis, A.; Martin, N.; Echegoyen, L.; Guldi, D. M. *Chem. Commun.* **2011,** 47, 2270-2272.
42.    Chen, N.; Pinzón, J. R.; Echegoyen, L. *ChemPhysChem* **2011,** 12, 1422-1425.
43.    Cardona, C. M.; Kitaygorodskiy, A.; Echegoyen, L. *J. Am. Chem. Soc.* **2005,** 127, 10448-10453.
44.    Cardona, C. M.; Kitaygorodskiy, A.; Ortiz, A.; Herranz, M. A.; Echegoyen, L. *J. Org. Chem.* **2005,** 70, 5092-5097.
45.    Perdew, J. P.; Burke, K.; Ernzerhof, M. *Phys. Rev. Lett.* **1996,** 77, 3865-3868.
46.    Laikov, D. N. *Chem. Phys. Lett.* **1997,** 281, 151-156.
47.    Laikov, D. N.; Ustynuk, Y. A. *Russ. Chem. Bull.* **2005,** 54, 820-826.
48.    Laikov, D. N. *Chem. Phys. Lett.* **2005,** 416, 116-120.
49.    Humphrey, W.; Dalke, A.; Schulten, K. *J. Molec. Graphics* **1996,** 14, 33-38.
50.    Popov, A. A.; Dunsch, L. *Phys. Chem. Chem. Phys.* **2011,** 13, 8977-8984.

TOC figure